Probing the Sub-microsecond Photodissociation Dynamics in Gas-Phase Retinal Chromophores

Lutz Lammich, Iben Bloch Nielsen, Hella Sand, Annette Svendsen, and Lars H. Andersen*

Department of Physics and Astronomy, University of Aarhus, DK-8000 Aarhus C, Denmark

Received: January 15, 2007; In Final Form: March 21, 2007

The photoinduced fragmentation of a retinal model chromophore (all-*trans*-*n*-butyl protonated Schiff-base retinal) was studied in vacuo using a new experimental technique. The apparatus is able to record the photodissociation yield of gas-phase biomolecular ions in the first microseconds after absorption. Together with the existing ion storage ring ELISA, which operates on the millisecond to second time scale, the complete decay dynamics of such molecules can now be followed. In the case of retinal, the time-dependent fragmentation yield observed after irradiation with a 410 nm laser pulse exhibits contributions from one- and two-photon absorption, which decay non-exponentially with lifetimes on the order of 1 ms and 1 μs, respectively. The decay can be simulated using a statistical model, yielding good agreement with the experimental findings on both the millisecond and the microsecond time scales. No indication for nonstatistical processes is found for this molecule, the upper limit for a possible direct rate being a factor of 10^4 below the observed statistical dissociation rate.

1. Introduction

Chromophores are the active centers of photosensitive proteins that play an important role in many biological organisms. They provide simple light-sensing abilities in small bacteria but are also the functional core of highly complex structures like the human visual system. Despite the variety of tasks performed by these proteins, such as recovery of energy, gathering of information on the surroundings, or signaling by re-emission of light, the first step in their photochemistry is always the absorption of light by the chromophore. The response of the chromophore molecule and its effect on the hosting protein then start a chain of events which eventually can result in a reaction by the whole organism.

A detailed understanding of chromophores and their interactions with the hosting proteins is of fundamental interest not only for describing the diverse examples of photoactive proteins found in nature but also for supporting microbiological applications, for example, of fluorescent proteins as markers. In a number of studies, different chromophores in various environments have thus been investigated, both experimentally and theoretically.[1−6]

An approach of particular importance for disentangling intrinsic chromophore properties from interactions with the environment is gas-phase studies. Here, model chromophores (commonly ions), which are not connected to a protein, are investigated in vacuum. Recent studies[1,7,8] have shown that this type of experiment is crucial for the understanding of the photoabsorption process since a variety of environmental perturbations like neighboring charges, hydrogen bonds, or steric constraints can lead to significant changes in the absorption properties, both in the protein and in the solution phase. Gas-phase experimental data are, therefore, highly desired as benchmarks for theoretical models.

Experiments on isolated chromophore ions, however, are challenging, as these species cannot be brought into the gas phase by standard ionization techniques without destroying the molecular structure. While this problem has been overcome with the advent of electrospray ion sources,[9] a remaining difficulty lies in the low ion density typically available in gas-phase experiments. Standard spectroscopic methods, which detect absorption as a change in transmission through a sample, are ruled out here since the dilute ion samples in gas-phase studies do not lead to a significant damping of the light intensity. Instead, such experiments may make use of action spectroscopy by detecting the response of the chromophores upon photoabsorption.

In general, the absorption of light by a chromophore in vacuum will, after the initial electronic excitation, lead to internal conversion of electronic energy into vibrational excitations, in essence, heat. This commonly results in a fragmentation of the molecule in a statistical process within the first milliseconds after photoabsorption, depending on the chromophore and the amount of energy absorbed (see section 3.5). A signature of absorption that may be used in action spectroscopy of gas-phase chromophores is thus the dissociation of the molecule, generally into both neutral and charged fragments, both of which can be detected depending on the specific experiment.

Apart from the statistical dissociation process, a much faster "prompt" fragmentation mode is conceivable, provided that a dissociative potential energy surface (PES) can be reached directly by photoabsorption.[10−12]

In this paper, we discuss a new technique which bridges the gap between the time scales of the statistical and prompt decay paths. We present an apparatus that is capable of following the photoinduced dissociation of chromophore ions over the first few microseconds after absorption by detecting neutral fragmentation products. This technique is sensitive to dissociation events taking place immediately after the photoabsorption with no dead time. On the other hand, the observation of chro-

* To whom correspondence should be addressed. E-mail: lha@phys.au.dk.

10.1021/jp070331z CCC: $37.00 © 2007 American Chemical Society
Published on Web 05/04/2007

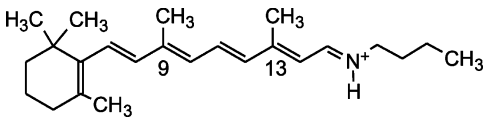

Figure 1. Structure of the all-*trans*-*n*-butyl protonated Schiff-base retinal model chromophore used in the present study.

mophores fragmenting several microseconds later enables us to relate this to experiments sensitive on much longer time scales.

We consider here the case of the retinal chromophore. This species is of special interest as it is found in a number of photoactive proteins, in particular those of the opsin class, which constitute the photoreceptors in the human eye.[13,14] Environmental interactions play an outstanding role here; in fact, it is the interaction of the same chromophore with three different hosting proteins which provides color vision. For a full understanding of the photophysics of retinal, it is therefore crucial to investigate its intrinsic properties in the gas phase. Concerning the absorption as a function of wavelength, a good agreement of the experimental spectrum[1,15] and theoretical calculations of the electronic transition energy[4,16] was recently reached.

The dynamics following the absorption in different environments are still under debate and subject to many experimental and theoretical studies (see, for example, refs 17−22). In the protein, the process of geometrical rearrangement of the chromophore on the excited S_1 surface, return to the S_0 ground state, and vibrational relaxation is assumed to take place on a time scale between several hundred femtoseconds and a few picoseconds.[19,20] On the other hand, a decay time of ∼33 ps was found for the return to the S_0 state in a nonpolar solvent.[21,22] Evidently, the environment plays an important role also concerning the dynamics after absorption. To see if the fast response in the protein is an intrinsic property of the chromophore or due to protein−chromophore interactions, gas-phase studies are needed again.

As a first step in determining the gas-phase photodynamics, we investigate here the possible role of a directly dissociative channel in the photofragmentation of retinal. To this end, we follow the fragmentation yield in a dead-time-free, time-resolved experiment on the sub-microsecond time scale. Complementing data in the millisecond regime are obtained using the ELISA storage ring[23], as described in section 3.4. The model chromophore employed in this work is all-*trans*-*n*-butyl retinal in the protonated Schiff-base form, as shown in Figure 1.

2. Experimental Setup

An overview of the experimental setup is shown in Figure 2. Chromophore molecules are dissolved in methanol, protonated by adding a small amount of acetic acid, and brought into the gas phase using an electrospray ion source.[23] Here, small charged droplets of the solution are formed by electrospray ionization. In a heated capillary, the solvent is then evaporated, and the remaining chromophore ions are collected in a Paul trap employing helium as a buffer gas. With a rate of 2 kHz, bunches of $\sim 10^2$ ions are extracted from the trap and accelerated to an energy of 20 keV. By passing a magnetic field of ∼0.5 T, ions of different mass-to-charge ratios are separated, yielding bunches of the desired protonated chromophore molecules. Using a switchable electrostatic deflector (chopper), the ions can be dumped onto an aperture, and for each trap filling, only a ∼0.4-μs-long subset of the ∼4 μs ion bunch is allowed to enter the laser interaction region.

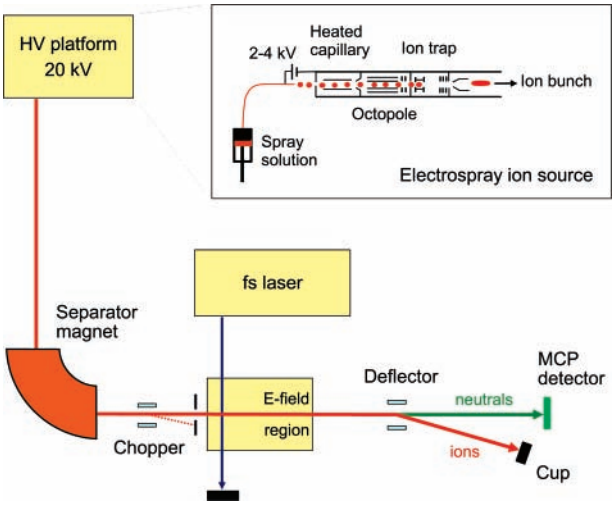

Figure 2. Schematic overview of the ion-beam and laser setup.

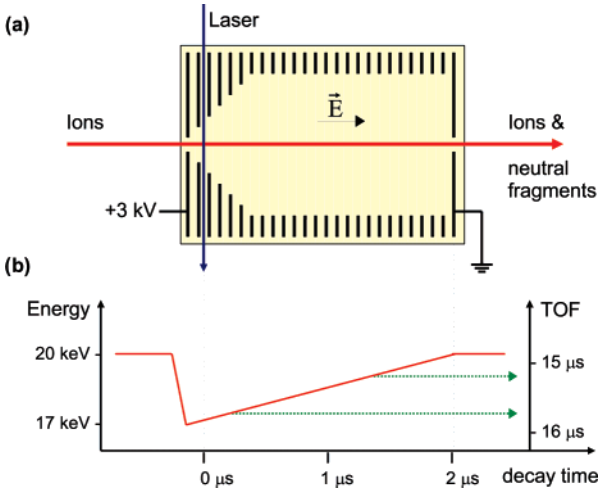

Figure 3. Use of the electric field region to resolve dissociation times: (a) a stack of electrodes is used to generate a homogeneous electric field; (b) the dissociation time of an ion is mapped to the time-of-flight of its neutral fragments through the varying beam energy over the length of the field region (see text for details).

Here, the ion beam is crossed with the frequency-doubled beam from a Ti:Sa femtosecond laser (wavelength $\lambda = 410$ nm, pulse duration 120 fs, pulse energy ∼0.15 mJ, repetition rate 1 kHz). The ion extraction from the Paul trap and the firing of the laser is synchronized such that every second ion bunch is hit by a laser pulse. Bunches, which are not exposed to laser light, are used to determine the amount of background dissociations in the residual gas.

After the interaction region, another electrostatic deflector is used to separate the ion beam from neutral fragments produced following photoabsorption or residual gas collisions. The neutrals are then registered by a microchannel plate (MCP) detector.

To investigate the dissociation times of the chromophore ions, that is, the time between the absorption of a photon and the emission of a neutral fragment, a stack of electrodes around the interaction region is used. As seen in Figure 3a, these electrodes create a homogeneous electric field, parallel to the ion-beam direction and covering the laser interaction point and ∼20 cm downstream. After abruptly reducing the kinetic energy of the ions when entering the field region, this field is slowly reaccelerating them and, hence, restoring the original beam

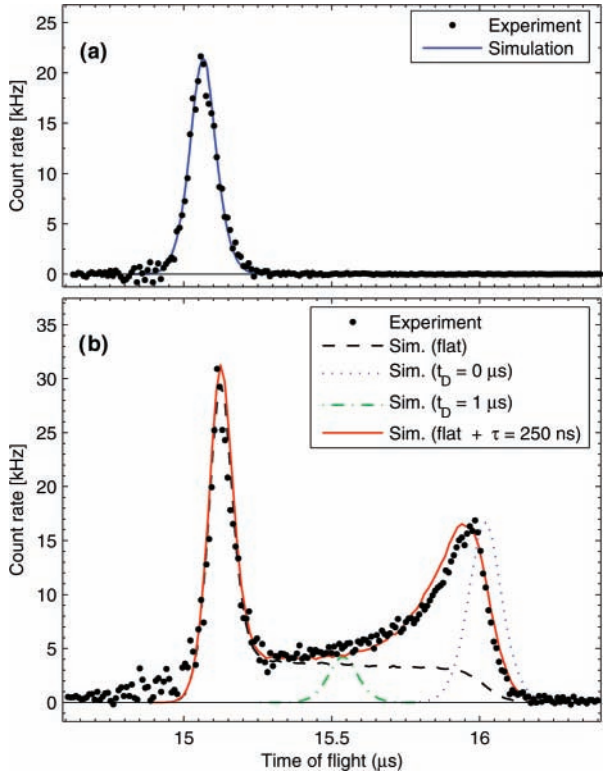

Figure 4. (a) TOF of photoinduced neutral fragments without applying an electric field. Full circles show experimental data for all-*trans*-*n*-butyl retinal chromophores taken at ~150 mW laser power ($\lambda = 410$ nm); the solid line is a simulated spectrum. (b) Results of the TOF measurement with the field applied. The lines here represent simulated data for different assumptions on the dissociation time t_D. Dashed line: random (flat) t_D distribution. Dotted line: $t_D = 0$ μs. Dash-dotted line: $t_D = 1$ μs. Solid line: 64% flat and 36% exponential decay with a lifetime of $\tau = 250$ ns.

energy at the exit of the field region (solid line in Figure 3b). Neutral fragments, which are formed during this reacceleration phase, will not be effected by the remainder of the accelerating field, and they thus continue their way to the detector at a reduced velocity, corresponding to the ion velocity at the time of the fragmentation (dotted arrows in Figure 3b). This reduced velocity manifests itself in an increased time-of-flight (TOF) of the neutral fragments from the laser interaction point to the MCP detector.

Using this procedure, the dissociation time of the chromophore ions can be determined through a measurement of the TOF of the neutral fragments produced. With the present experimental parameters, dissociation times up to 1.6 μs can be resolved for retinal ions, while ions with a dissociation time of 1.6−3.8 μs will all exhibit the same TOF since they fragment in the field-free region after the E-field region. Ions with an even longer dissociation time will reach the deflector before fragmenting and thus become invisible to the MCP detector.

3. Results

3.1. Time-of-Flight Spectrum. Figure 4 shows the TOF spectrum obtained for photofragmentation of all-*trans*-*n*-butyl retinal chromophores in the protonated Schiff-base form. Contributions due to residual gas collisions have been subtracted. In Figure 4a, the parallel electric field was turned off, whereas in Figure 4b, a voltage of +3 kV was applied. Without the field, the TOF spectrum exhibits a single peak at ~15.05 μs. The spread in TOF observed here stems from several effects including small fluctuations in the ion-beam energy, the transverse extension of the laser beam, and in particular, the velocity gained or lost by neutral fragments through the kinetic energy released in the dissociation process.

When applying the electric field (Figure 4b), this peak essentially remains unaffected, except for a small shift toward longer TOF. The events piled up here have dissociation times t_D between 1.6 and 3.8 μs and thus dissociate in the field-free region after the E-field, that is, at the full beam velocity. The small shift is a result of the additional time spent in the field region due to the lower beam energy here. In addition, a second peak structure extending to a TOF of 16 μs is observed, corresponding to a considerable fraction of ions with very low t_D, which dissociate within the field region.

To interpret the measured spectrum, a Monte Carlo simulation algorithm was developed, which is able to predict the TOF spectrum resulting from a given t_D distribution taking into account the geometry of the experiment. This algorithm first generates a set of dissociation times according to the assumed t_D distribution. Furthermore, the initial ion-beam energy and the laser interaction point are generated for each event from the narrow distribution of acceleration voltages and the laser beam profile. Using these data, the position of each dissociation event along the ion-beam axis can be calculated. At this point, the fragment velocity is calculated from the local ion-beam energy and modified according to the assumed velocity distribution of the neutral fragments in the co-moving center-of-mass frame of the chromophore ions. Knowing the velocity of the neutral fragments, the time-of-flight from the point of dissociation to the MCP detector can be determined and thus the total TOF as measured between the laser interaction and the impact on the detector.

The additional velocity distribution, which stems from the kinetic energy released isotropically in the fragmentation process, is the dominating contribution to the spread in TOF. It is thus determining the experimental resolution and has to be reproduced by the simulation algorithm. For an empirical determination of this contribution, experimental and simulated data are compared for the case where the electric field around the interaction region is switched off (Figure 4a), and thus, the TOF spectrum consists of a single peak with a shape determined by the distribution of velocities obtained in the fragmentation process. While the identity of the neutral fragments cannot be determined in the present experiment, their kinetic energy is estimated to be ~0.7 eV per atomic mass unit based on the simulation results.

The simulation algorithm can now be used for a closer inspection of the experimental data shown in Figure 4b; the dashed line shows the simulated TOF spectrum resulting for a flat (random) distribution of dissociation times within the time window of 0−3.8 μs accessible in the experiment. The assumption of, for example, an exponential decay with a time constant in the millisecond range, similar to that measured previously at ELISA,[1] would yield essentially the same picture here. The high rate in the experimental data at up to 16 μs thus clearly indicates an additional, short-lived contribution to the decay of the chromophores.

The resolution and sensitivity of the experiment is illustrated by the dotted and dash-dotted lines, which show simulation results for fixed dissociation times of $t_D = 0$ and 1 μs, respectively. The temporal evolution of the photofragmentation can be followed up to $t_D \sim 1.6$ μs with a resolution on the order of 0.1 μs.

In an attempt to mimic the full experimental spectrum, another simulation was performed, which assumes a randomly distrib-

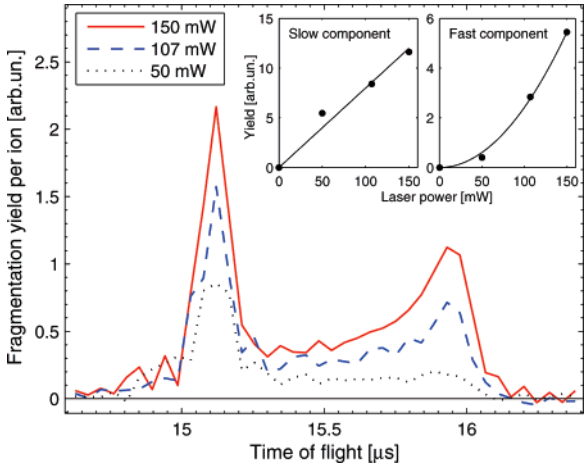

Figure 5. Laser power dependence. The main graph shows the TOF spectrum recorded at three different laser powers, as given in the legend. The contributions of slow and fast decay components to the spectrum can be extracted (see text) and are plotted in the insets. Fitting a second-order polynomial reveals a purely linear (quadratic) dependence of the slow (fast) component on the laser power.

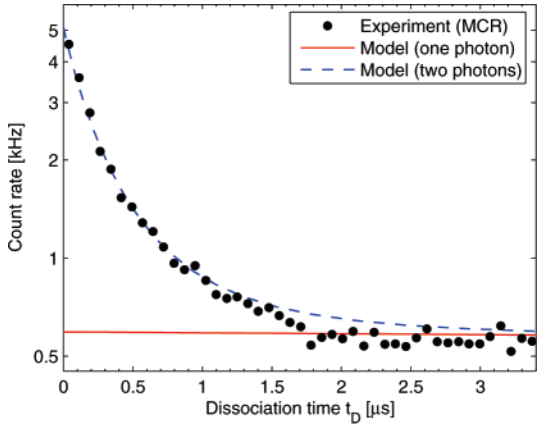

Figure 6. Short component of the photoinduced decay rate. Circles: results of a Monte Carlo restoration from the measured TOF spectrum (Figure 4). Lines: statistical model of the decay after one-photon (solid line) and two-photon (dashed line) absorption.

uted dissociation time for 64% of the events, while for the remaining 36%, an exponential decay with a lifetime of 250 ns was used. The resulting TOF spectrum (solid line in Figure 4) shows good overall agreement with the experimental data. The remaining deviations suggest a slightly non-exponential character of the short time decay component, but the time scale of the decay is well reproduced. In particular, no additional contribution stemming from even shorter time scales (below ~10 ns) is found, which would manifest itself in a peak similar to the dotted curve in Figure 4.

3.2. Laser Power Dependence. To shed more light on the nature of the fast decay component, the dependence of the TOF spectrum on the laser power, measured after the interaction region, was studied (see Figure 5). To account for different acquisition times and ion-beam intensities in the three measurements, each of the data sets was normalized to the number of background counts recorded without laser light. The resulting normalized rate is thus proportional to the laser-induced fragmentation yield per ion.

As is evident from the three TOF spectra, a reduction of the laser power suppresses the fast decay component (TOF ~ 16 μs) more strongly than the slow component (TOF ~ 15.1 μs). The magnitude of the two contributions can be extracted from the data by assuming that the fast component has largely died out after $t_D \sim 1$ μs and that the slow component is approximately flat in t_D, that is, the shape of its TOF spectrum corresponds to the dashed line in Figure 4. By comparing the number of events recorded before and after a TOF of, for example, 15.4 μs, the total yield attributed to the slow and fast component, respectively, can now be extracted at each laser power (insets in Figure 5). A fit to a second-order polynomial (with the zeroth-order term set to zero) yields a purely linear power dependence for the slow component, while for the fast component, a purely quadratic dependence is found.

The obvious conclusion is that the observed fast decay component originates from absorption of two photons from the same laser pulse. Importantly, no evidence for a fast (sub-microsecond) dissociation channel accessible after one-photon absorption is found.

Our discussion until now made no conclusions as to whether the fast decay after two-photon absorption is due to a more direct decay channel accessible at higher excitation energy or due to the same statistical fragmentation process that governs the breakup after one-photon absorption. To address this question, a more detailed analysis of the decay curves after both one- and two-photon absorption is given in the following.

3.3. Monte Carlo Restoration of the Dissociation Time Distribution. On the basis of the algorithm described in section 3.1, which simulates the instrumental response for each dissociation time, a Monte Carlo restoration (MCR) technique[24] can be applied in order to reconstruct the underlying dissociation time distribution from a measured TOF spectrum. This method starts by randomly choosing dissociation times within the range visible in the experiment. The events generated in this way are then run through the simulation algorithm to yield a set of TOF values. From these values, a simulated TOF histogram is constructed, adding events one by one and rejecting any event that would cause the corresponding bin in this histogram to exceed the value seen in the experimental TOF histogram. Eventually, the constructed histogram will reproduce the experimental TOF spectrum, and at the same time, the dissociation times of all simulated events that were accepted in this process will represent the deconvoluted dissociation time distribution. Naturally, such an unfolding procedure cannot be completely unambiguous, and in particular, it cannot overcome the limit set by the resolution of the $t_D \rightarrow$ TOF transformation.

This method provides a representation of the experimental results in terms of a dissociation time histogram, which is consistent with the measured TOF histogram. While keeping in mind its limitations, the t_D distribution can still be used to study the main features of the time dependence of the two-photon fragmentation process. Figure 6 shows the t_D spectrum obtained using the MCR method together with a statistical decay model, which will be described in section 3.5.

3.4. Millisecond Decay Dynamics Observed at ELISA. The major part of the photoinduced fragmentation of chromophore ions takes place on the millisecond time scale and is thus only partly accessible in the present experiment. However, it can be studied using the ELectrostatic Ion Storage ring Aarhus, ELISA.[23,25] In this ring, ions produced by an electrospray ion source are stored up to several seconds at beam energies of typically 22 keV. The ions are irradiated in the ring by a nanosecond laser using a merged-beams geometry. Employing a MCP detector sensitive to neutral fragments leaving the ring, the decay of the excited ions can then be followed as a function of time for various laser wavelengths. Recent experiments on retinal model chromophores are described in refs 1,15,26.

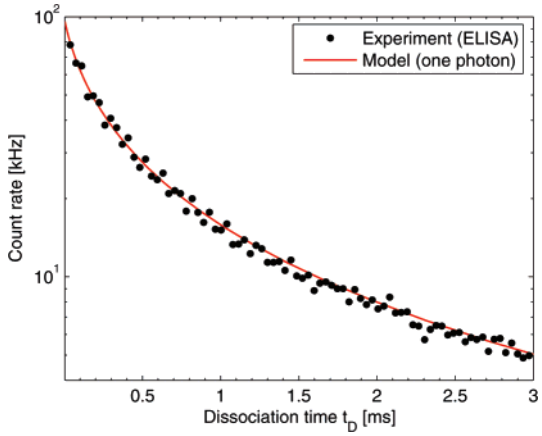

Figure 7. Long component of the photoinduced decay rate. Circles: experimental data from ELISA (wavelength 397 nm, pulse duration 30 ns). Solid line: statistical model of the decay after one-photon absorption.

For comparison with the short time data discussed here, Figure 7 shows a dissociation time spectrum recorded at ELISA using the same type of chromophores and a similar laser wavelength.

3.5. Comparison to a Statistical Decay Model. In order to reproduce the observed time dependence of the chromophore fragmentation, a statistical model based on an Arrhenius-type over-the-barrier mechanism is used, as described in detail in refs 6 and 27. In short, this model assumes, as a first step, the internal conversion of the absorbed energy into vibrational excitations. Through a fast intramolecular vibrational redistribution (IVR) process, a thermal distribution of the energy among the vibrational modes of the chromophore is then reached. The molecule is considered to fragment once the energy stored in a particular mode (corresponding to the cleavage of the weakest bond) exceeds an activation energy E_A. The fragmentation process is then accounted for by the Arrhenius law

$$k = A \cdot \exp\left(-\frac{E_A}{k_B T^*}\right)$$

where k is the fragmentation rate for a molecule with a particular initial energy. The pre-exponential factor A basically describes how frequently the molecule attempts to overcome the barrier to dissociation due to its vibrational motion, k_B is the Boltzmann constant, and T^* the emission temperature of the system during the fragmentation process (that is, the microcanonical temperature of the chromophore after absorption, corrected for the finite heat bath, see ref 27 for details).

The fragmentation yield I as a function of time can then be calculated, also taking into account the distribution $G(E)$ of initial energies of the chromophore ions

$$I(t) = \int \mathrm{d}E G(E) k \exp(-kt)$$

For the ion sources used here, the initial ion energies are estimated to be thermally distributed with a temperature around 500 K. For the transformation between temperature and internal energy, the heat capacity $C_V(E)$ of the chromophore is needed, which is derived from the vibrational frequencies obtained from a Gaussian98 calculation at the PM3 level of theory.[28]

The modeled time dependence of the fragmentation yield can now be compared to the experimental results for one- and two-photon absorption. The lines in Figures 6 and 7 show results of the statistical model for a parameter choice of $E_A = 2.0$ eV and $A = 2 \times 10^{16}$ s^{-1}. Since, in both experiments, the number of ions irradiated by each laser pulse is not known on an absolute scale, only a relative comparison of the shape of the decay curves is possible. To this end, the modeled rate in Figure 7 was scaled by a factor adjusted to fit the overall level of the experimental data. Apparently, the time scale and shape of the decay curve are very well reproduced by the model with this choice of parameters.

In Figure 6, the scale of the modeled one-photon contribution was set to fit the constant level of the MCR results at $t_D = 1.9-3.8$ μs, stemming from the peak at 15.1 μs in the TOF spectrum. For the two-photon contribution, the model was scaled to match the experiment at shorter times. Evidently, the measured decay curve at the microsecond time scale can be described by the same statistical model as that for millisecond times using the same values for the parameters E_A and A. In this situation, the relative contribution of one- and two-photon absorption to the total decay rate can be extracted from the scale factors used in Figure 6, yielding a two-photon contribution of 0.3% at a laser-pulse energy of 150 μJ. As a consequence, the strength of a possible direct, nonstatistical decay can only be on the order of $\sim 10^{-4}$ or less compared to the slow statistical decay after one-photon absorption.

Considering the systematic uncertainties regarding, for example, the initial ion temperature or the resolution of the TOF measurement, these results should not be interpreted as an accurate determination of E_A and A. However, the good agreement of the model with the experimental data on both time scales clearly shows that the concept of an entirely statistical decay of the retinal chromophore is consistent with the experimental findings. The values obtained for E_A and A are comparable to those found for other chromophores.[6] The order of magnitude of A furthermore indicates that retinal does not dissociate via a highly ordered transition state, in contrast to, for example, anionic model chromophores of the red fluorescent protein (RFP), where the formation of an additional ring structure was observed.[6]

4. Conclusions

We presented an experimental setup which allows for the observation of the photofragmentation of chromophore ions on a time scale of a few microseconds, with full sensitivity down to zero dissociation time and a resolution well below 1 μs. The application of this technique on a retinal model chromophore completes the decay curve, which was measured for decay times from $\sim$40 μs up to several milliseconds in previous experiments. The full decay curve could be described by a statistical decay model. In other words, no decay path resulting in an instantaneous photodissociation of this molecule was found, even though 410 nm light was used, which allows the excitation of the second excited state of the chromophore.[1]

Since part of the signal measured on the microsecond time scale stems from two-photon absorption, pump−probe experiments appear feasible with the same apparatus. For this purpose, the setup will be upgraded to allow for an excitation of the chromophore ions by two femtosecond laser pulses with variable wavelength and time delay. These pump−probe studies will then enable us to follow the dynamics preceding the dissociation on a femtosecond time scale.

Acknowledgment. This work was supported by the Lundbeck Foundation and the Danish Natural Science Research Council (Grant # 21-03-0330).

References and Notes

(1) Nielsen, I. B.; Lammich, L.; Andersen, L. H. *Phys. Rev. Lett.* **2006**, *96*, 018304.
(2) Freedman, K. A.; Becker, R. S. *J. Am. Chem. Soc.* **1986**, *108*, 1245.
(3) Cembran, A.; González-Luque, R.; Altoè, P.; Merchán, M.; Bernardi, F.; Olivucci, M.; Garavelli, M. *J. Phys. Chem. A* **2005**, *109*, 6597.
(4) Sekharan, S.; Weingart, O.; Buss, V. *Biophys. J.* **2006**, *91*, L07.
(5) Röhrig, U. F.; Guidoni, L.; Rothlisberger, U. *ChemPhysChem* **2005**, *6*, 1836.
(6) Andersen, L. H.; Bluhme, H.; Boye, S.; Jorgensen, T. J. D.; Krogh, H.; Nielsen, I. B.; Brøndsted Nielsen, S.; Svendsen, A. *Phys. Chem. Chem. Phys.* **2004**, *6*, 2617.
(7) Brøndsted Nielsen, S.; Lapierre, A.; Andersen, J. U.; Pedersen, U. V.; Tomita, S.; Andersen, L. H. *Phys. Rev. Lett.* **2001**, *87*, 228102.
(8) Lammich, L.; Andersen, L. H.; Petersen, M. Å.; Brøndsted Nielsen, M. *Biophys. J.* **2007**, *92*, 201.
(9) Fenn, J. B.; Mann, M.; Meng, C. K.; Wong, S. F.; Whitehouse, C. M. *Science* **1989**, *246*, 64.
(10) Schlag, E. W.; Selzle, H. L.; Schanen, P.; Weinkauf, R.; Levine, R. D. *J. Phys. Chem. A* **2006**, *110*, 8497.
(11) Grégoire, G.; Kang, H.; Dedonder-Lardeux, C.; Jouvet, C.; Desfrançois, C.; Onidas, D.; Leperec, V.; Fayeton, J. A. *Phys. Chem. Chem. Phys.* **2005**, *8*, 122.
(12) Brøndsted Nielsen, S.; Andersen, J. U.; Forster, S.; Hvelplund, P.; Liu, B.; Pedersen, U. V.; Tomita, S. *Phys. Rev. Lett.* **2003**, *91*, 048302.
(13) Wald, G. *Science* **1968**, *162*, 230.
(14) Terakita, A. *GenomeBiology* **2005**, *6*, 213.
(15) Andersen, L. H.; Nielsen, I. B.; Kristensen, M. B.; Ghazaly, M. O. A. E.; Haacke, S.; Brøndsted Nielsen, M.; Petersen, M. Å. *J. Am. Chem. Soc.* **2005**, *127*, 12347.
(16) Bochenkova, A. V.; Granovsky, A. A.; Bravaya, K. B.; Nemukhin, A. V. *J. Chem. Phys.* **2006**, submitted.
(17) Kim, J. E.; Tauber, M. J.; Mathies, R. A. *Biophys. J.* **2003**, *84*, 2492.
(18) Kukura, P.; McCamant, D. W.; Yoon, S.; Wandschneider, D. B.; Mathies, R. A. *Science* **2005**, *310*, 1006.
(19) Abramczyk, H. *J. Chem. Phys.* **2004**, *120*, 11120.
(20) Schenkl, S.; van Mourik, F.; Friedman, N.; Sheves, M.; Schlesinger, R.; Haacke, S.; Chergui, M. *Proc. Natl. Acad. Sci. U.S.A.* **2006**, *103*, 4101.
(21) Tahara, T.; Hamaguchi, H. *Chem. Phys. Lett.* **1995**, *234*, 275.
(22) Ishii, K.; Takeuchi, S.; Tahara, T. *Chem. Phys. Lett.* **2006**, *418*, 307.
(23) Andersen, J. U.; Hvelplund, P.; Brøndsted Nielsen, S.; Tomitaa, S.; Wahlgreen, H.; Møller, S. P.; Pedersen, U. V.; Forster, J. S.; Jørgensen, T. J. D. *Rev. Sci. Instrum.* **2002**, *73*, 1284.
(24) Frieden, B. R. In *Picture Processing and Digital Filtering*; Huang, T. S., Ed.; Topics in Applied Physics; Springer-Verlag: Berlin, Germany, 1975; Vol. 6, p 177.
(25) Møller, S. P. *Nucl. Instrum. Methods Phys. Res., Ser. A* **1997**, *394*, 281.
(26) Petersen, M. Å.; Nielsen, I. B.; Kristensen, M. B.; Kadziola, A.; Lammich, L.; Andersen, L. H.; Brøndsted Nielsen, M. *Org. Biomol. Chem.* **2006**, *4*, 1546.
(27) Andersen, J. U.; Bonderup, E.; Hansen, K. *J. Chem. Phys.* **2001**, *114*, 6518.
(28) Frisch, M. J.; Trucks, G. W.; Schlegel, H. B.; Scuseria, G. E.; Robb, M. A.; Cheeseman, J. R.; Zakrzewski, V. G.; Montgomery, J. A., Jr.; Stratmann, R. E.; Burant, J. C.; Dapprich, S.; Millam, J. M.; Daniels, A. D.; Kudin, K. N.; Strain, M. C.; Farkas, O.; Tomasi, J.; Barone, V.; Cossi, M.; Cammi, R.; Mennucci, B.; Pomelli, C.; Adamo, C.; Clifford, S.; Ochterski, J.; Petersson, G. A.; Ayala, P. Y.; Cui, Q.; Morokuma, K.; Malick, D. K.; Rabuck, A. D.; Raghavachari, K.; Foresman, J. B.; Cioslowski, J.; Ortiz, J. V.; Stefanov, B. B.; Liu, G.; Liashenko, A.; Piskorz, P.; Komaromi, I.; Gomperts, R.; Martin, R. L.; Fox, D. J.; Keith, T.; Al-Laham, M. A.; Peng, C. Y.; Nanayakkara, A.; Gonzalez, C.; Challacombe, M.; Gill, P. M. W.; Johnson, B. G.; Chen, W.; Wong, M. W.; Andres, J. L.; Head-Gordon, M.; Replogle, E. S.; Pople, J. A. *Gaussian 98*, revision A.9; Gaussian, Inc.: Pittsburgh, PA, 1998.